atmosphere

MDPI

Article

Supplementary material for Cyclones signature in the South-West of Indian Ocean from two decades of microseismic noise

Elisa J. Rindraharisaona [1,2,*], Guilhem Barruol [1], Emmanuel Cordier [3] and Fabrice R. Fontaine [1,2,4] and Alicia Gonzalez [1,2,5]

1 Université de Paris, Institut de physique du globe de Paris, CNRS, F-75005 Paris, France
2 Université de La Réunion, Laboratoire GéoSciences Réunion, F-97744, Saint Denis, France
3 Observatoire des Sciences de l'Université de La Réunion, UMS3365 (CNRS, Université de La Réunion, Météo-France), Saint-Denis de La Réunion, France
4 Observatoire volcanologique et sismologique de la Martinique, Institut de physique du globe de Paris, F-97250 Fonds Saint Denis, France.
5 Université de Bourgogne/Franche-Comté - CNRS UMR 6249 Chrono-Environnement 16, route de Gray F-25030 Besançon Cedex France.
* Correspondence: elisa.rindraharisaona@univ-reunion.fr

check for updates

Citation: Rindraharisaona, E.J.; Barruol, G.; Cordier, E.; Fontaine, F.R.; Gonzalez, A. Supplementary material for Cyclones signature in the South-West of Indian Ocean from two decades of microseismic noise. *Atmosphere* **2021**, *12*, 488. https://doi.org/10.3390/atmos12040488

Academic Editor: Olivier Bousquet

Received: 29 January 2021
Accepted: 5 April 2021
Published: 13 April 2021

Publisher's Note: MDPI stays neutral with regard to jurisdictional claims in published maps and institutional affiliations.

S1. Computation of the polarization coefficients

To determine the degree of rectilinearity, the polarization coefficients (CpH and CpZ) see [1], the three components of the ground motion were used (see section 2.2). The polarization coefficient in the horizontal plane CpH is obtained from the covariance matrix calculated from the horizontal components, which is defined by

$$CpH = 1 - \frac{\lambda_{min}^{NE}}{\lambda_{max}^{NE}},$$

where λ_{NE}^{min} and λ_{max}^{NE} correspond to the minimum and maximum eigenvalues, obtained from the covariance matrix calculated from the horizontal components.

To determine the polarization coefficient in the vertical plane CpZ, we first rotated the North and East-West components, using the back-azimuth to obtain the longitudinal component. The CpZ is then obtained from the covariance matrix from the longitudinal and vertical components defined by

$$CpZ = 1 - \frac{\lambda_{min}^{LZ}}{\lambda_{max}^{LZ}},$$

where λ_{min}^{LZ} and λ_{max}^{LZ} correspond to the minimum and maximum eigenvalues, calculated from the covariance matrix of the longitudinal and vertical components.

S2. Transfer functions PM amplitude and significant wave height H_S

Giovanna (Figure S6a) has an interesting trajectory to study correlation between the PM and the local H_S. Giovanna formed as a Tropical Disturbance (TD) on February 2, 2012, and evolved to an Intense Tropical Cyclone (ITC) as it passed at the northern side of the island between February 12 and late 13. During this period (within the black dashed lines), we obtain P_{coef} of 0.93, 0.94 and 0.95 at the NW, N and NE nodes, respectively (Figure S6b), and the computed and modelled H_S were in agreement within 1 m (Figure S6e). However, difference between the modeled and estimated H_S are >2 m between late February 13 to 16, during which Giovanna continued its journey westward and was overland Madagascar on February 14 and in the western side of Madagascar until February 16. Plausible explanation of the discrepancy observed here is that PM may be generated by distant-swell (possibly

generated by Giovanna earlier on February 13) that travelled southward. Such swell may have interacted with the local bathymetry at the western side of the nodes plotted here (hence the absence of GOW2 H_S). Alternatively, the apparent shift between the peaks in the modeled H_S and the observed PM may indicate that the south-western coast of the island has been affected about one day later by strong waves not reproduced by the model. This could suggest a H_S underestimation by the numerical model on Feb. 14. It may also indicate that the observed microseismic amplitude here are associated to a LPSM of period >10, generated on the continental shelf in a relatively deep water at large distance from the seismic station as hypothesized e.g., [2,3]. After February 17, Giovanna retrieves a "normal" behaviour; it travelled eastward over the ocean south of Madagascar and made a swift northward early on February 20, and again passed at the western and northern side of La Réunion between February 21 and 22. During the passage of Giovanna at the north and west sides of La Réunion, PM amplitude and H_S were strengthened simultaneously, and the modelled and estimated H_S retrieved comparable values (for the nodes $W1$, $W2$ and NW).

For cyclones that still have energy when drifting southward from the island, H_S appeared to be often overestimated by the fact that one observes peaks of large seismic amplitudes which poorly correlate with modelled H_S. This observation is clear for Felleng (February 2 to 4, 2013, Figure S6f), Imelda (April 14 to 18, 2013, Figure S6g), Berguitta (January 19 to 22, 2018, Figure S7f) and Dumazile (March 7 to 10, 2018 Figure S7g). Such behaviour may result from weakness in the H_S model or, more likely, that the measured RMS are related to more distant sources such as a (LP)SM (Long Period Secondary Microseism), with period >10 s, as suggested by the daily power spectral densities for these cyclones in Figure S9.

Cyclone Bansi (Figure S7e) provides another type of anomaly, with unexpectedly low seismic PM signal. From January 11 to 15, 2015, Bansi was categorized as TC and ITC and was still at the northern side of the island. However, despite the presence of high $P_{coef} > 0.8$ at the northern nodes, the computed H_S appear to be underestimated. This low PM level can be due to the fact that despite the strength of the cyclone (wind >250 km/h), waves may not develop accordingly due to a fetch not long enough. The observed weak PM may also result from the attenuation of the cyclonic waves from the storm center before interacting with the local bathymetry. The discrepancy between the modelled and estimated H_S that starts on January 16 could be due to the fact that the waves interacted with the local bathymetry at the south-western sides of the nodes plotted here. Figure **??**i shows that the maximum H_S between January 16 and 20 corresponds to the node at 55.00°E21.50°S (south-western node). The observed PM is most likely generated by the cyclone Chedza, which passed at the south-western side of island ($<$ 500 km) between January 17 and 19.

Tables

Table 1. SWIO terminology for tropical-system classification with respect to wind intensity. More details about the classification and nomination can be found at http://www.meteo.fr/temps/domtom/La_Reunion/webcmrs9.0/anglais/index.html and in Leroux *et al.* [4].

Type	Mean Maximum Wind, V_{max} (Km/h)
Zone of Disturbed Weather & Tropical Disturbance	$V_{max} \leq 50$
Tropical Depression (TD)	$50.0 < V_{max} \leq 62.6$
Moderate Tropical Storm (MTS)	$62.6 < V_{max} \leq 88.6$
Severe Tropical Storm (STS)	$88.6 < V_{max} \leq 118.4$
Tropical Cyclone (TC)	$88.6 < V_{max} \leq 118.4$
Intense Tropical Cyclone (ITC)	$V_{max} \geq 166.7$

Figures

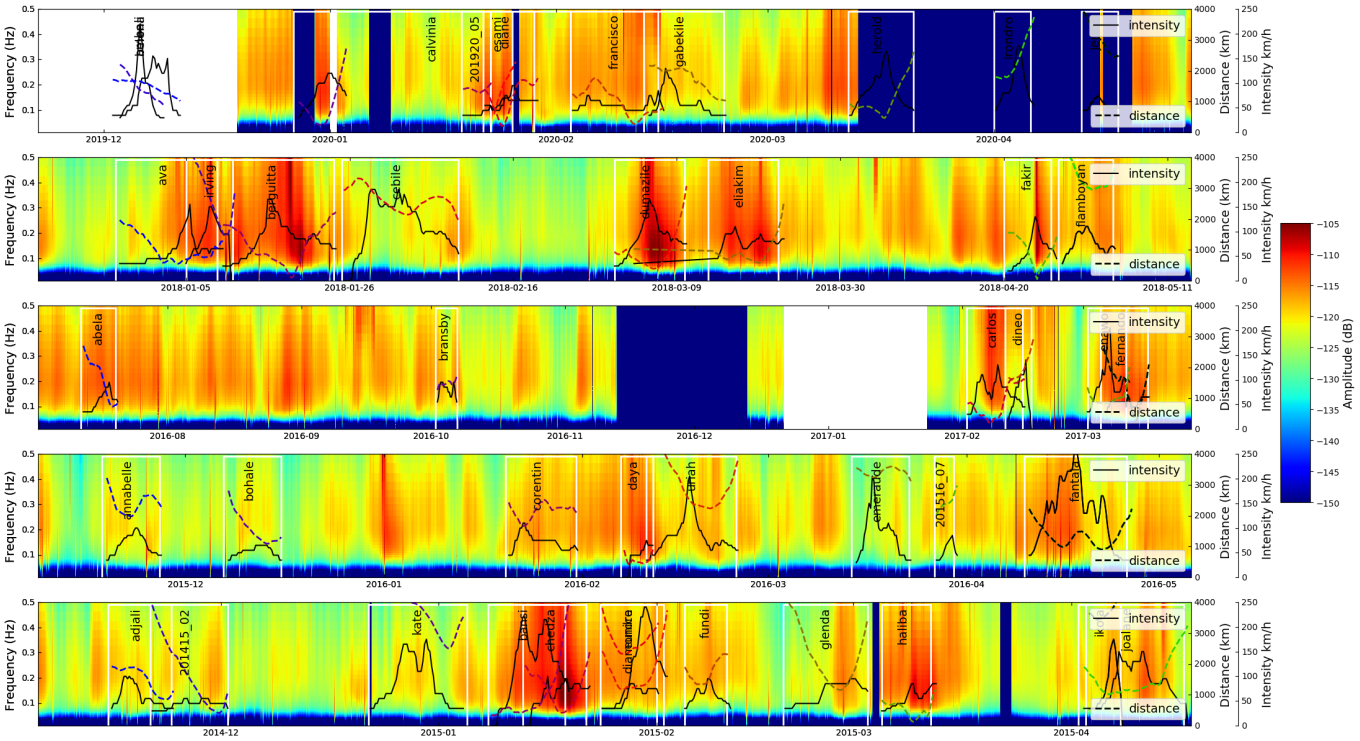

Figure S1. Spectrogram of microseismic noise at RER seismic station (vertical component) for the cyclonic season 2014-2020. Each cyclone is indicated by a white box. Black lines show the cyclone's intensity (right axis, showing the wind velocity in km/h from MF) and colored dashed lines show the distance between the storm center and RER station.

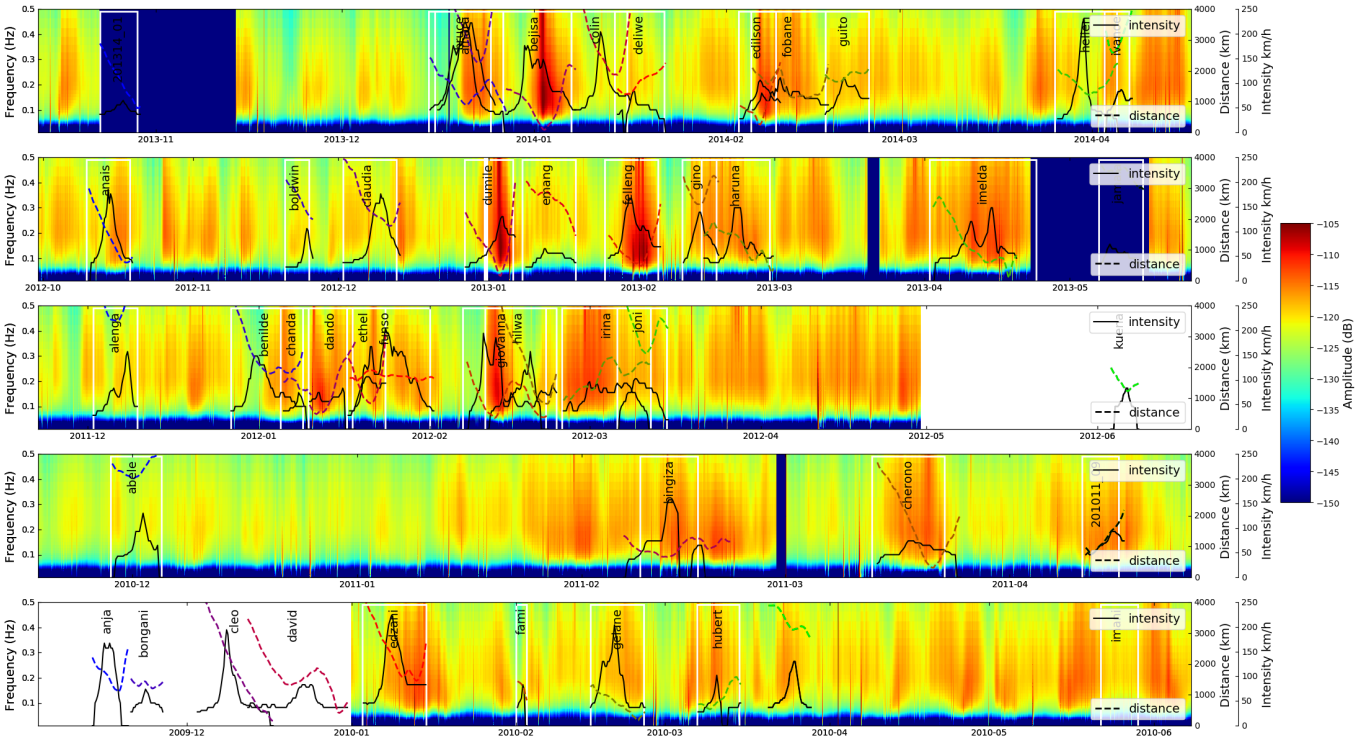

Figure S2. Same as S1 but for 2009 to 2013.

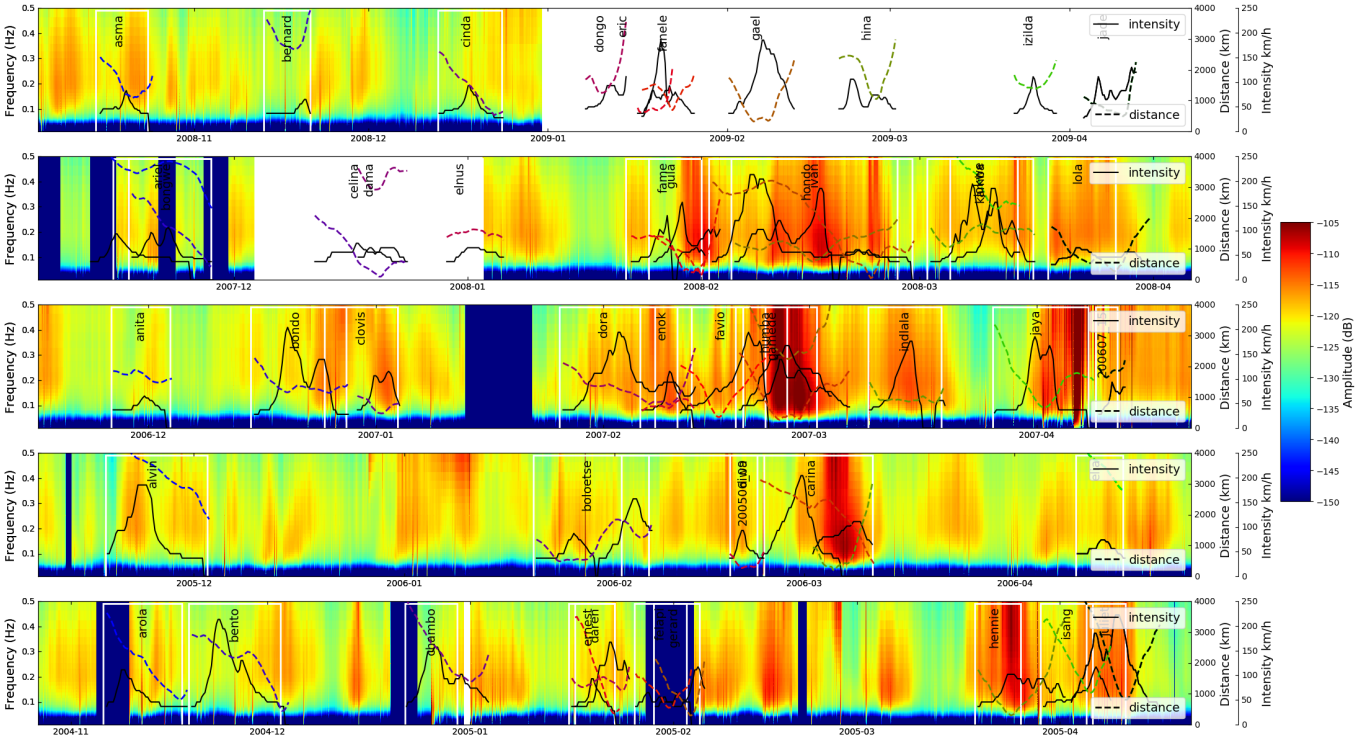

Figure S3. Same as S1 but for 2004 to 2008.

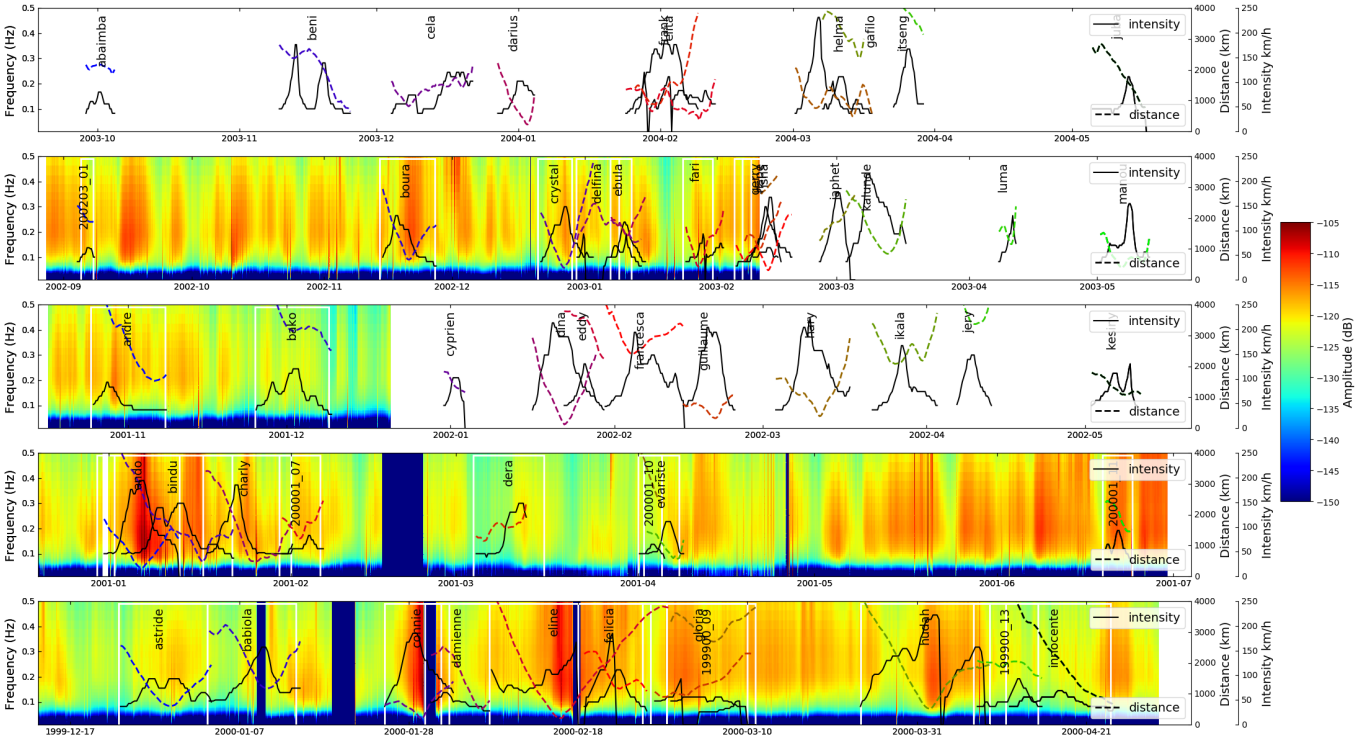

Figure S4. Same as S1 but for 1999 to 2003.

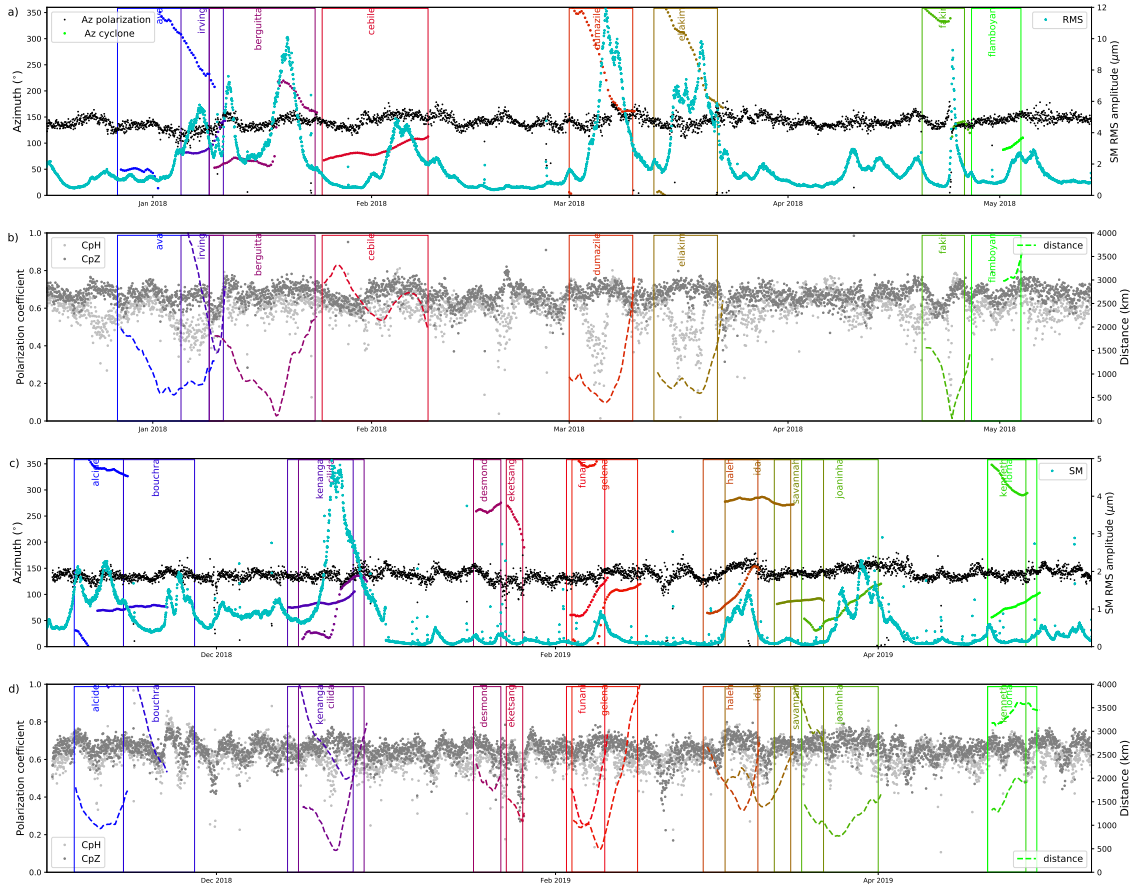

Figure S5. Cyclone polarisation analysis. **a, c)** Comparison of the theoretical BAZ issued from the TC center provided by MF (colored dots, 6 hours step) with our measured BAZ from the polarization analysis (black dots, hourly average) of RER seismic data, for the cyclonic seasons between 2017-2018 **(a)** and 2018-2019 **(c)**. The SM amplitude are plotted in dotted cyan colors. The distance between the seismic station RER and the storm center are plotted in dashed colored lines. The corresponding trajectories and intensities of the cyclones are plotted in Figure 6. **b, d)** An hourly polarization parameters *CpH* (light gray dots) and *CpZ*(dark gray dots) in the SM frequency band. The distance between the storm center and the RER are plotted in dashed color lines.

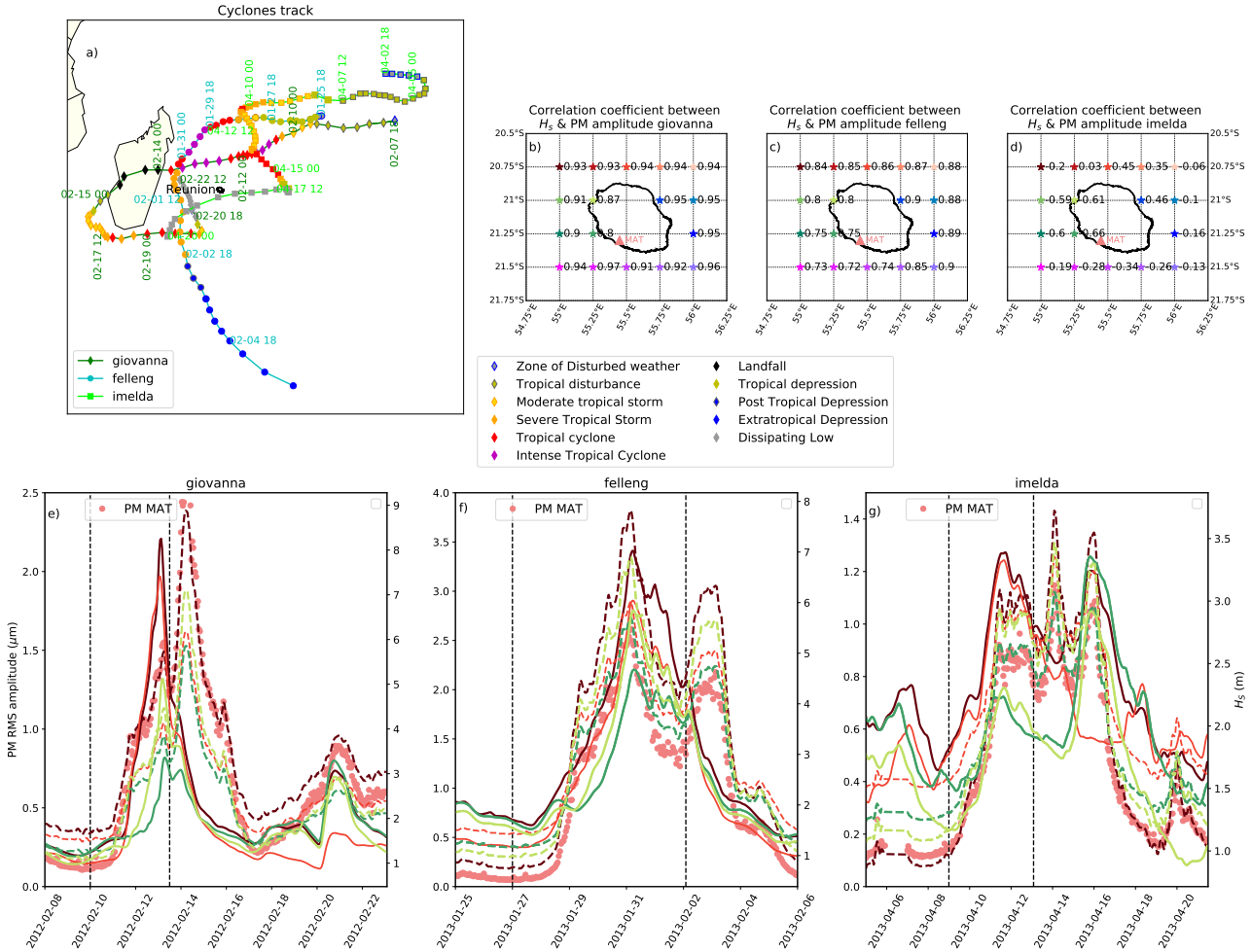

Figure S6. a): PM and HS correlations. Trajectories of Giovanna (Feb. 2012, diamonds), Felleng (Jan. 2013, dots) and Imelda (Apr. 2013, squares) and their respective correlation coefficient with the H_S in **b)**, **c)** and **d)**. The colors of the different symbols in map a) are plotted according to the cyclone intensity (see the legend on the lower right side). To avoid overcrowded of the map, only the month, day and hour plotted on the maps. **e)**, **f)** and **g):** For each cyclone, the PM amplitude measured at station MAT (pink dots) are plotted together with the GOW2 model [5] (continuous lines) and estimated (using the transfer functions for the corresponding nodes, dashed lines) H_S. The vertical dashed lines indicate the date limit use to compute the coefficient correlations.

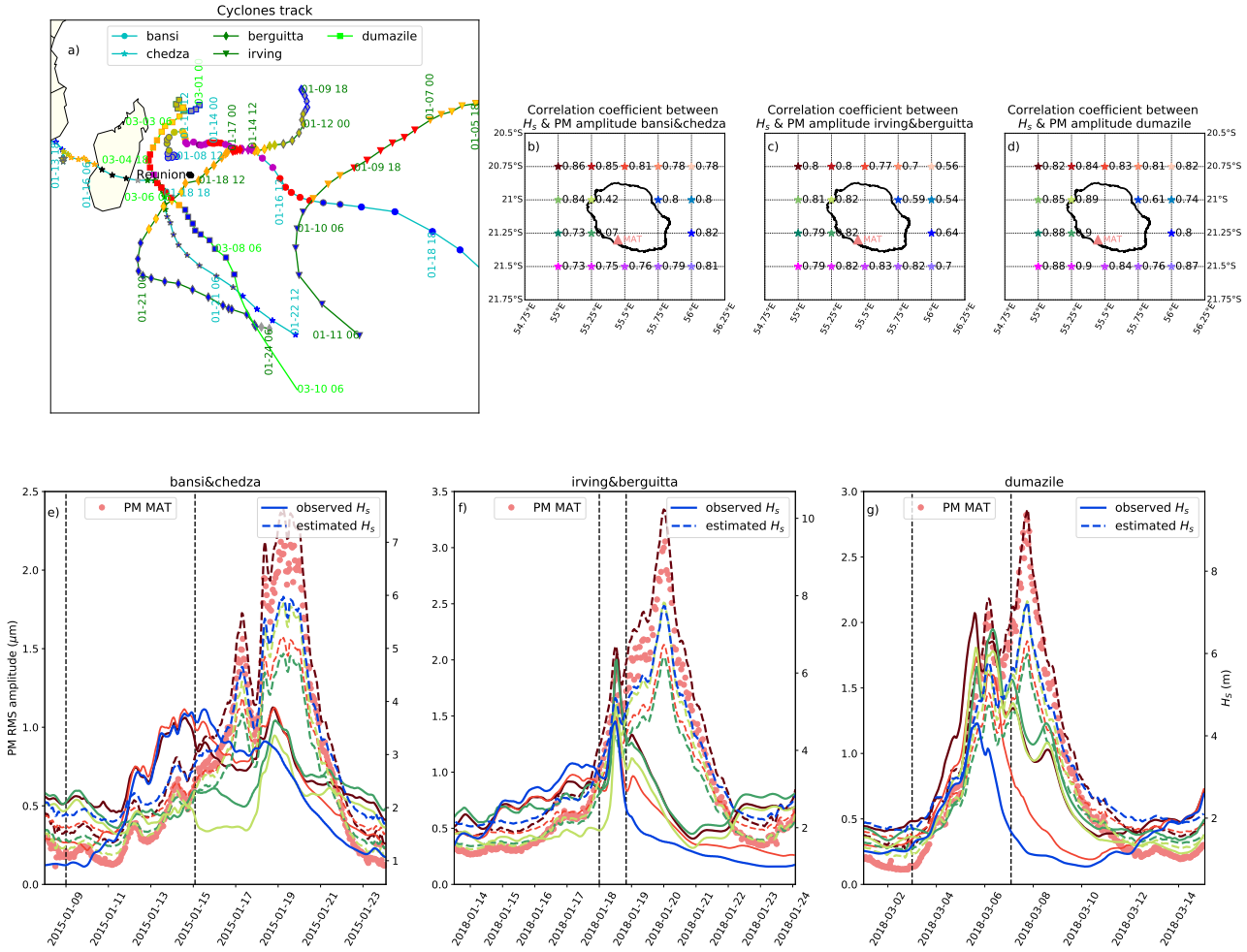

Figure S7. Same as S6 but for Bansi & Chezda (Jan. 2015, dots & star symbols), Irving & Berguitta (Jan. 2018, inverse triangles & diamonds symbols) and Dumazile (Mar. 2018, squares symbol).

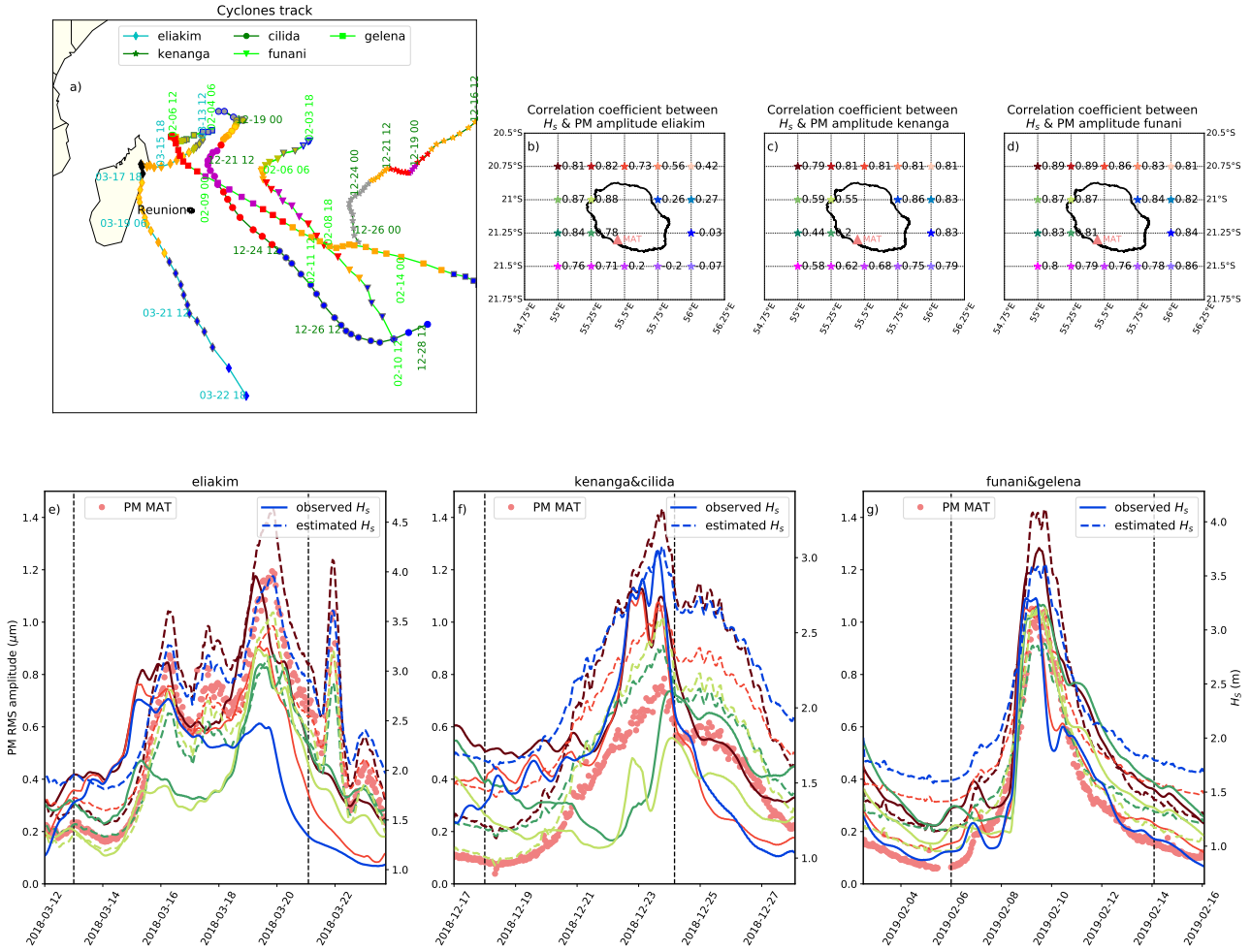

Figure S8. Same as S6 but for Eliakim (Mar. 2018, diamonds symbol), Kenanga & Cilida (Dec. 2018, stars & dots symbols) and Funani & Gelena (Feb. 2019, inverse triangles & diamonds symbols).

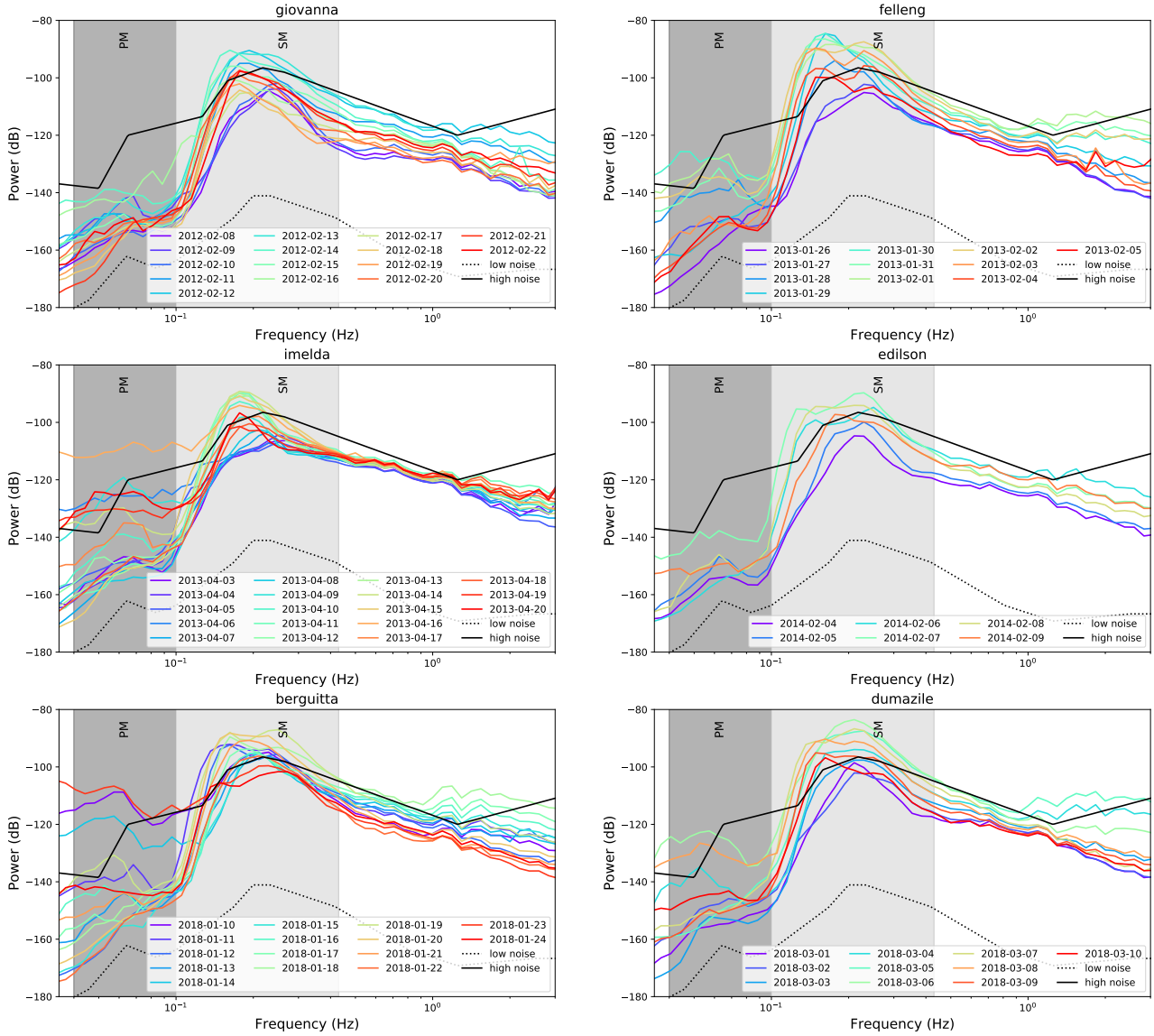

Figure S9. Evolution of the daily power spectral density for Giovanna, Felleng, Imelda, Edilson, Berguitta and Dumazile.

References

1. Flinn, E. Signal analysis using rectilinearity and direction of particle motion. *Proceedings of the IEEE* **1965**, *53*, 1874–1876. doi:10.1109/PROC.1965.4462.
2. Ardhuin, F.; Gualtieri, L.; Stutzmann, E. How ocean waves rock the Earth: Two mechanisms explain microseisms with periods 3 to 300s. *Geophysical Research Letters* **2015**, *42*, 765–772. doi:10.1002/2014GL062782.
3. Hasselmann, K. A statistical analysis of the generation of microseisms. *Reviews of Geophysics* **1963**, *1*, 177–210. doi:10.1029/RG001i002p00177.
4. Leroux, M.D.; Meister, J.; Mekies, D.; Dorla, A.L.; Caroff, P. A climatology of southwest Indian Ocean tropical systems: their number, tracks, impacts, sizes, empirical maximum potential intensity, and intensity changes. *Journal of Applied Meteorology and Climatology* **2018**, *57*, 1021–1041.
5. Perez, J.; Menendez, M.; Losada, I.J. GOW2: A global wave hindcast for coastal applications. *Coastal Engineering* **2017**, *124*, 1–11. doi:10.1016/j.coastaleng.2017.03.005.